

RESEARCH ARTICLE

The Soft Layer Thickness Estimation using Microtremor Measurement to Identify Landside Potential in Watukumpul, Central Java, Indonesia.

Urip Nurwijayanto Prabowo^{1,*}, Akmal Ferdiyan¹, Ayu Fitri Amalia²

¹Physics Department, Faculty of Mathematics and Natural Science, Universitas Jenderal Soedirman, Purwokerto, Indonesia.

²Physics Education Department, Faculty of Teacher Training and Education, Universitas Sarjanawiyata Tamansiswa, Yogyakarta, Indonesia.

* Corresponding author : urip.np@unsoed.ac.id

Tel.:(0281) 638793

Received: Aug 10, 2020; Accepted: March 17, 2021.

DOI 10.25299/jgeet.2021.6.1.5436

Abstract

Watukumpul is an area that is prone to landslides, so determining the soft layer thickness is very important to identify the landslide potential. The soft layer thickness can be estimated using microtremor signal measurements which analyzed using the Horizontal to Vertical Spectral Ratio (HVSr). In this study, we measured microtremor signal of 33 location around Watukumpul, Pemalang, Central Java area to determine soft layer thickness. Microtremor signal was analyzed based on the HVSr method using Geopsy software and follow the standard of the Sesame European Project. The results of the HVSr method are the HVSr curve that fulfills the reliable curve standard. HVSr curve shows that the dominant frequency of soft layer ranges from 1.36 – 7.62 Hz and the amplification values ranges from 9.00 – 41.45. The soft layer thickness value in the study area ranges from 17.58 - 103.60 meters. The high landslide potential area are located at W7, W8, W18, W30 and W32 where has thin soft layer and high soil slope.

Keywords: Microtremor, HVSr, Soft layer thickness

1. Introduction

Watukumpul is an area in the south of Pemalang Regency, Central Java. Watukumpul is an area that has the potential to experience landslides because it is a hilly area with a high soil slope (Prabowo et al., 2019), so a sustainable mitigation effort is needed. Landslide as a process of soil or rock movement due to disturbing slope equilibrium (Suhendra et al., 2018). Several parameters that influence the occurrence of landslides are soil type, volume of unstable soil / soft layer (Firmansyah et al., 2016), landslide slip surface (Darsono et al., 2016), and other parameter. In this study, we conducted preliminary survey to determine location where has a high potential volume of unstable soil based on the soft layer thickness estimation in Watukumpul. However, the soft layer thickness also reflect the depth of landslide slip surface.

The geotechnical and geophysical method can be used to estimate the soft layer thickness, i.e. borehole drilling, geoelectricity method (Islami, 2019), SASW method (Naing et al., 2015), array-microtremor (Koesuma et al., 2017; Liu et al., 2014) and Microtremor measurement (Seht and Wohlenberg, 1999; Supriyadi et al., 2019). In this study, we estimate the soft layer thickness using microtremor measurement which analyzed using Horizontal to

Vertical Spectral Ratio (HVSr) method. Microtremor measurement was proven beneficial to give a wider picture of subsurface ground investigation due to non-destructive, reliable, and cost-effective method (Kamarudin et al., 2016). Microtremor measurement also useful to get a subsurface information of the shallow and deep soil layer (Kyaw et al., 2015)

Microtremor is the constant vibrations of the earth with a very small amplitude, and the displacements are in the order of 10^{-4} to 10^{-2} mm (Okada, 2003). The microtremor signal analysis using the HVSr method was developed by Nakamura in 1989. This method calculated the spectrum ratio of the microtremor signal in a horizontal component to its vertical component. The results of the HVSr method analysis are the HVSr curve, which the curve peak related to the dominant frequency and amplification values that describe the site response characteristic or local site effect (Anggono et al., 2016; Nakamura, 2008). Dominant frequency and amplification can also be used to determine the weak zone of an area that has the potential to experience damage during an earthquake (Sulistiawan et al., 2017) and the response of soft surface surfaces when experiencing an earthquake (Yulianto et al., 2016). Besides that, the dominant frequency value describes the thickness of the surface sediment layer (Zulfakriza et al., 2019). Other research states that the HVSr method is

efficiently used in determining the contact boundary between stable and unstable material in landslides (Méric et al., 2007)

2. The Study Area

The study area is located in the south of Pemalang regency and near the Slamet Mountain. Watukumpul is a downhill area with high soil slope. Fig 1 of the Watukumpul geological map, which shows that the

study area consists of Rambatan formation and Halang formation with some diorite intrusion. Halang formation consists of andesitic sandstone, tuffaceous conglomerate, and marl intercalates with sandstone. While Rambatan formation consists of shale, marl, and calcareous sandstone (Djuri et al., 1996).

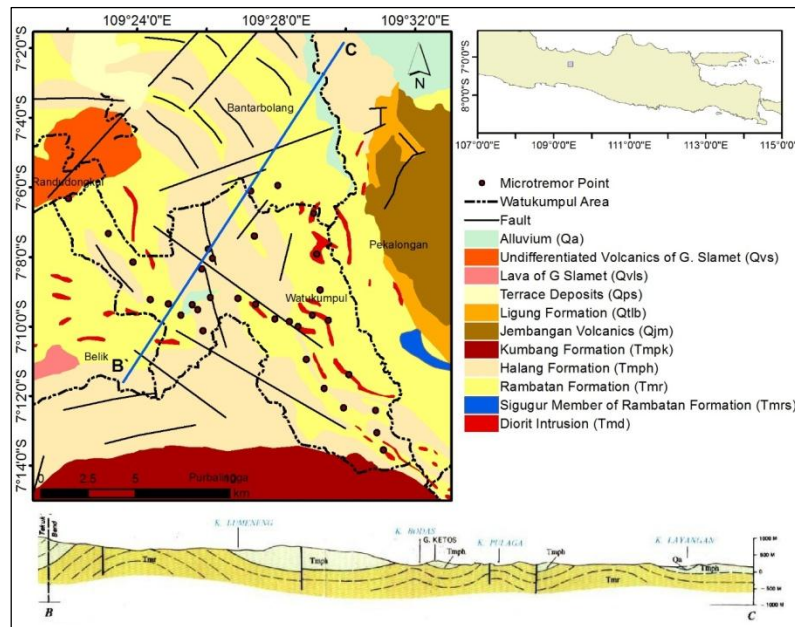


Fig. 1. Geological map of the study area (black dotted is microtremor measurement location) (Modified after Djuri et al., 1996).

3. Methodology

3.1 Data Acquisition

Microtremor signals were recorded at 33 locations in Watukumpul Pemalang (Fig 1). The microtremor signal was recorded using a three-component seismometer type of MAE with a sampling rate of 100 Hz. Measurement was carried out in a quiet location to minimize noise. The measurement duration, for each point was about 20 minutes.

In this research, we also used shear wave velocity at a depth of 30 meters (V_{s30}), which was obtained from the United States Geological Survey (USGS).

3.2 Horizontal to Vertical Spectral Ratio (HVSr)

Horizontal to Vertical Spectral Ratio (HVSr) is a 3-component microtremor data analysis method. In this study, the microtremor signal processing using Geopsy software, and the standard criteria for data processing according to the Sesame European Project.

The HVSr method begins with manually selected the stationary signal by windowing the signal with a window width of the 20s. Then, the microtremor signal in the time domain was transformed into the frequency domain through the Fast Fourier Transform (FFT) process with a tapering value of 5% and subsequently smoothen using the Konno-Omachi method with a constant value of $b = 40$ (SESAME European Research Project, 2004). The result of the spectrum on the horizontal component ($H(f)$) divided

by the vertical component ($V(f)$) based on Equation (1) to obtain the HVSr curve (Nakamura, 2008).

$$HV - ratio = \frac{H(f)}{V(f)} = \frac{\sqrt{H_{EW}^2(f) + H_{NS}^2(f)}}{V(f)} \quad (1)$$

Where $H_{EW}(f)$ is a spectrum of the horizontal component in the east-west direction, and $H_{NS}(f)$ is a spectrum of horizontal components in the north-south direction

The peak of the HVSr curve shows the dominant frequency and amplification values.

3.3 The Soft Layer Thickness

The soft layer thickness is related to the dominant frequency, which is the resonant frequency of the surface sediment layer when it reaches the maximum amplification value. The relationship between thickness and dominant frequency can be determined based on the closed Organa pipe rule. The maximum amplitude in close Organa pipe occurs when the thickness is a quarter of the wavelength (Seht and Wohlenberg, 1999). So the soft layer thickness can be determined using equation (2)

$$f_0 = \frac{V_s}{4H} \quad (2)$$

where f_0 is dominant frequency, V_s is shear wave velocity of soft layer and H is the thickness of soft layer. In this study we used V_{s30} data as the input of V_s parameter

4. Result and Discussion

4.1 HVSR Results

The result of microtremor signal analysis using the HVSR method is the HVSR spectrum curve. The HVSR curves of some locations show two curve peaks (Fig 2) which means there are two dominant frequencies. The two peaks of the HVSR curve show that the microtremor signal at the time of measurement captured two subsurfaces impedance contrasts from the deep and shallow soil layers (Kyaw et al., 2015). The dominant frequency of microtremor measurements does not necessarily indicate the characteristics of a single layer due to the complex ground vibration motion (Thein et al., 2013).

Further analysis was carried out on the HVSR curve which met the criteria for a reliable curve, as follows in Figure 3. Based on criteria in Fig 3, we can conclude that all the HVSR spectrum curve fulfill the criteria for a reliable curve. The fulfillment of first criteria based on the dominant frequency value of the first peak (1.36 – 7.62 Hz) which higher than the criteria $\frac{10}{I_w} = 0.5$ (window length is 20 s). The second criteria was fulfilled by all the HVSR curve because all the point has more than 10 number of windows so the significant number of cycles were than 200. The third criteria is fulfilled because no HVSR curve has standard deviation of amplitude more than 2.

Table 1. HVSR Result and the soft layer thickness from HVSR first peak (H)

No	Microtremor Point	Long (deg)	Lat (deg)	First Peak		Second Peak		$V_{S_{30}}$	H (m) (from first peak)	Geological formation
				A_0	f_0	A_i	f_i			
1	W1	109.37	-7.11	15.94	1.60	-	-	438.58	68.40	Rambatan Formation
2	W2	109.39	-7.12	15.98	2.92	-	-	715.23	61.28	Rambatan Formation
3	W3	109.40	-7.14	16.87	2.62	-	-	693.03	66.10	Rambatan Formation
4	W4	109.41	-7.15	21.61	1.90	15.82	7.65	609.06	79.97	Rambatan Formation
5	W5	109.41	-7.16	11.63	2.14	11.82	6.50	569.81	66.47	Rambatan Formation
6	W6	109.42	-7.16	12.73	1.64	26.10	7.25	579.81	88.22	Rambatan Formation
7	W7	109.43	-7.17	11.81	3.40	19.64	5.84	649.75	47.82	Rambatan Formation
8	W8	109.43	-7.13	21.17	6.90	-	-	606.30	21.97	Halang Formation
9	W9	109.44	-7.13	14.68	3.35	18.25	7.27	583.38	43.57	Halang Formation
10	W10	109.43	-7.14	31.04	7.62	-	-	536.25	17.58	Halang Formation
11	W11	109.43	-7.15	34.65	2.63	-	-	540.53	51.30	Halang Formation
12	W12	109.43	-7.16	12.34	1.36	-	-	563.19	103.60	Alluvium
13	W13	109.43	-7.16	41.45	4.11	-	-	570.62	34.69	Alluvium
14	W14	109.47	-7.10	14.84	6.04	-	-	508.60	21.04	Halang Formation
15	W15	109.45	-7.10	20.93	6.48	-	-	496.39	19.15	Rambatan Formation
16	W16	109.46	-7.12	15.43	3.44	-	-	639.23	46.40	Halang Formation
17	W17	109.45	-7.15	35.53	5.25	17.50	15.42	565.52	26.91	Rambatan Formation
18	W18	109.46	-7.16	36.13	6.87	-	-	583.28	21.23	Rambatan Formation
19	W19	109.47	-7.16	23.45	6.57	-	-	598.59	22.78	Diorit Intrusion
20	W20	109.47	-7.16	12.86	6.85	-	-	589.90	21.53	Rambatan Formation
21	W21	109.48	-7.16	32.87	2.65	-	-	548.26	51.74	Rambatan Formation
22	W22	109.48	-7.17	11.67	3.04	60.78	18.09	587.20	48.32	Rambatan Formation
23	W23	109.48	-7.18	15.35	3.24	-	-	609.86	47.03	Diorit Intrusion
24	W24	109.49	-7.20	13.37	2.61	14.77	5.61	653.75	62.64	Rambatan Formation
25	W25	109.50	-7.21	19.38	2.46	18.62	5.75	632.91	64.43	Rambatan Formation
26	W26	109.48	-7.11	23.57	1.91	-	-	514.28	67.49	Rambatan Formation
27	W27	109.49	-7.13	14.84	2.23	-	-	461.15	51.70	Diorit Intrusion
28	W28	109.49	-7.15	23.75	2.30	29.75	7.25	490.77	53.44	Diorit Intrusion
29	W29	109.49	-7.16	20.40	4.24	-	-	547.10	32.26	Rambatan Formation
30	W30	109.50	-7.19	11.59	2.47	10.36	5.92	629.12	63.60	Rambatan Formation
31	W31	109.51	-7.21	19.68	2.57	20.84	11.82	657.49	63.86	Diorit Intrusion
32	W32	109.51	-7.22	14.46	2.24	18.47	5.39	683.85	76.43	Halang Formation
33	W33	109.52	-7.23	9.00	2.18	-	-	665.65	76.41	Halang Formation

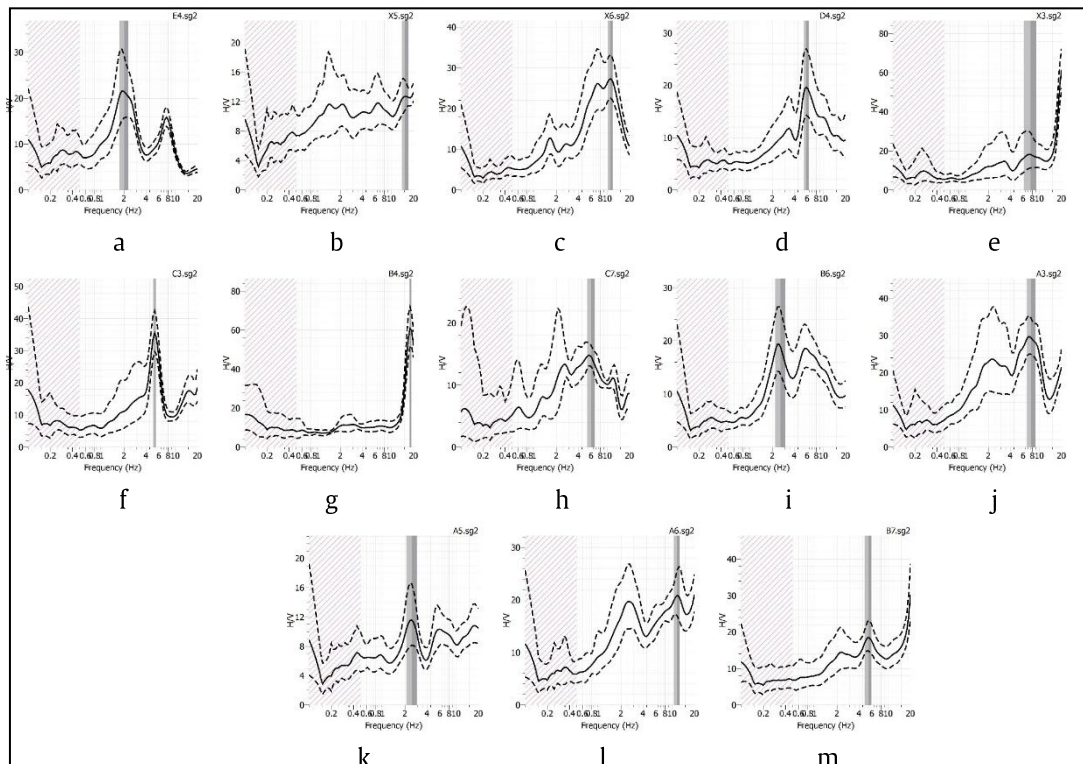


Fig 2. HVSR curve with 2 peaks (a) W4; (b) W5; (c) W6; (d) W7; (e) W9; (f) W17;(g) W22; (h) W24; (i) W25; (j) W28; (k) W30; (l) W31; (m) W32

Criteria for a reliable HVSR curve	
1.	$f_0 > \frac{10}{I_w}$
2.	$n_c(f_0) > 200; n_c(f_0) = I_w \cdot n_w \cdot f_0$
3.	$\sigma_A(f) < 2$ for $0,5f_0 < f < 2f_0$ if $f_0 > 0.5$ or $\sigma_A(f) < 2$ for $0,5f_0 < f < 2f_0$ if $f_0 > 0.5$ with f = frequency f_0 = dominant frequency I_w = window length n_w = number of windows n_c = number of significant cycles σ_A = standard deviation of HVSR dominant frequency

Fig 3. Criteria for a reliable HVSR curve (SESAME European Research Project, 2004)

Table 1 showed the dominant frequency and amplification value of reliable HVSR curve. The HVSR results used for further analysis were the dominant frequency at the first peak, which reflected the deep soft layer and present at all measurement points. The amplification value of the first peak ranged from 9.00 – 41.45 (Fig. 4). Amplification value provides information about the potential effect of earthquake vibration resonance on buildings so it can correlate with local ground shaking characteristics (Stanko et al., 2019). The high amplification value located at central of watukumpul so this area has the higher potential of earthquake vibration resonance effect. The threshold of amplification and frequency value (seismic

vulnerability index) which caused earthquake damage can be determined by correlate the value with the earthquake damage map (Daryono et al., 2009). But in this study, we could not determine the threshold because there are no data about earthquake damage history.

The amplification value describes the geological conditions between the sediment layer and the hard rock which beneath it and does not correlate with the dominant frequency or thickness of the soft layers (Prabowo et al., 2018). The high amplification value is located in the middle of the study area, dominated by sandstone of the Halang formation with an age ranged between late Miocene and Pliocene. The high amplification value caused by younger and softer rocks in the Halang formation than rocks layer below from Rambatan formation (middle Miocene age) (Fig. 1). In other areas where consisted of rock from Rambatan formation, the amplification value is relatively small because the soft layer formed from weathered rock of the Rambatan formation so the difference conditions between the sediment layer and the hard rock is small.

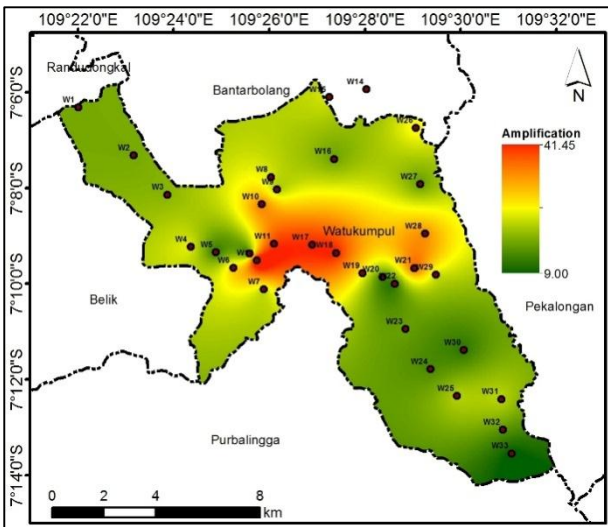


Fig 4. Amplification map

The dominant frequency of HVSR curve first peak ranged from 1.36 - 7.62 Hz (Fig. 5). The frequency value is proportional to the thickness of the soft sediment layer. A high dominant frequency value is located in the middle of the study site which is composed of rocks from the Halang formation and little part of the Rambatan formation. This high frequency value indicates a thinner sediment layer in the middle of the study area than the other measurement areas.

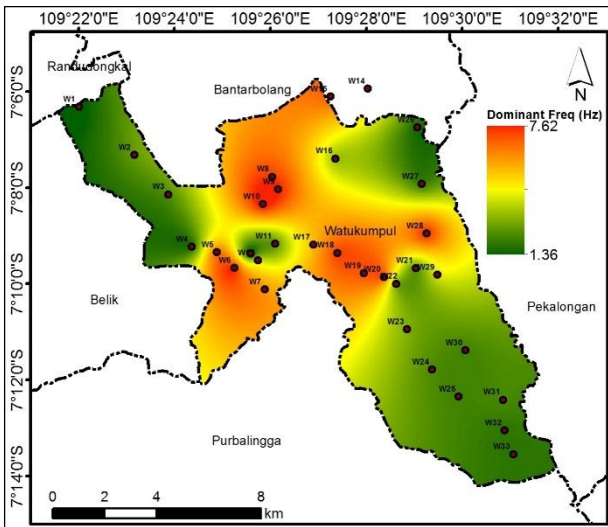


Fig 5. Dominant frequency map

4.2 The Soft Layer Thickness of Study Area

The soft layer thickness in the study area is determined based on equation (2) with the calculation results shown in Table 1 and Fig 6. The thickness of the soft layer in the Watukumpul area ranges from 17.58 - 103.60 meters.

Fig 3 shows the distribution of location and the thickness of the soft layer in the study area. The thicker soft sediment layer is located in the west of the study area at point W1 - W6, which ranges from 61.28 - 88.22 meters, and the largest value is at point W12 which is 103.60 meters. Thicker soft layer is also located in the southern area of the area at points W30 - W31, which ranges from 63.60 - 76.43 meters.

Figure 7 shows that point W12 has the largest thickness of the sediment layer composed of alluvium deposits with quarter age. The thick accumulation of alluvium probably originates from a higher area at the west of point W12. Point W12 is in an area with low elevation and tends to be flat so that the soft soil tends to be stable. This indicates that the potential for landslides is very small even though the thickness of the sediment is the largest.

In Figure 7, points W4 and W5 have the potential for landslides. This is due to the high elevation with a large soil slope and slip surface. The rocks at this location are dominated by sandstone from Halang formation with a large soft soil thickness ranging from 66 - 80 m

Figure 8 shows a cross section of the thickness of the sediment layer from north to south. In the northern area, it tends to have an even thickness of soft soil and a relatively small slope, so the potential for landslides is low. The southern area has a large enough soil elevation and slope with a thickness of soft soil between 63 - 76 m. This causes the southern area to have the potential for landslides. At point W32 it is composed of rocks from the Halang formation which are between the tougher Rambatan formations. This allows the geometry of the slip plane in the form of curves under the Halang formation which can trigger rotational landslides.

Figures 7 and 8 show that the thickness of the soft soil can provide a preliminary picture of the volume of soft soils and the morphology of the slip plane. The potential for large landslides is in locations with thick soft soil and large soil slopes. Based on land slope data in previous studies, locations with large soil slopes and thickness of sediment layers shown in Fig9. There were 5 point; W7, W8, W18, W30, and W32 which has land slide potential. These point has soil slope more than 20° and the soft soil thickness ranged between 21.2 - 76.4 m. The highest soil slope is $29,14^\circ$ which located in W8. The landslide potential assessment in this study was limited in 33 measurement point location. There another location with higher soil slope that have not measure yet caused by our limitation in time, transportation acces and facilities.

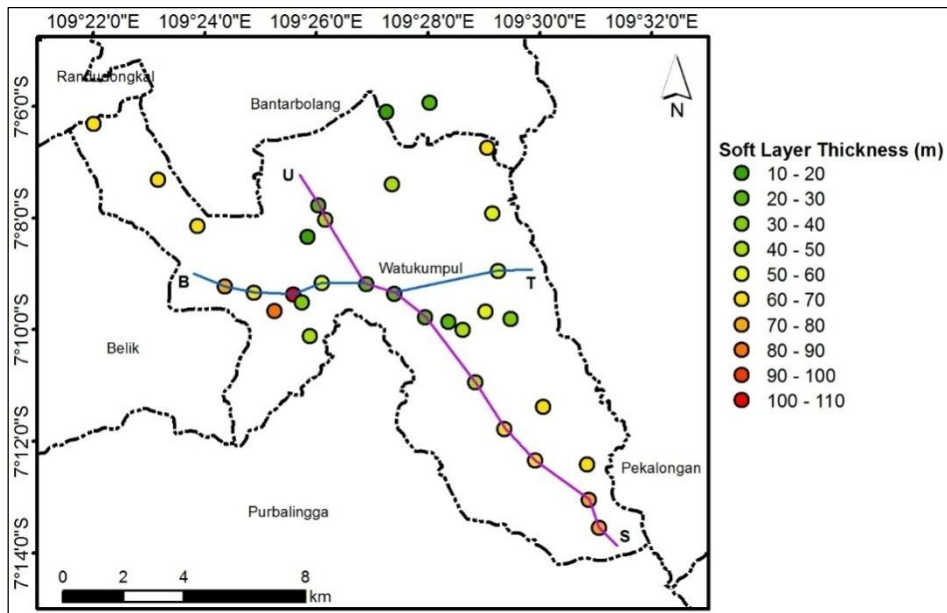


Fig. 6. Map of the Soft layer thickness

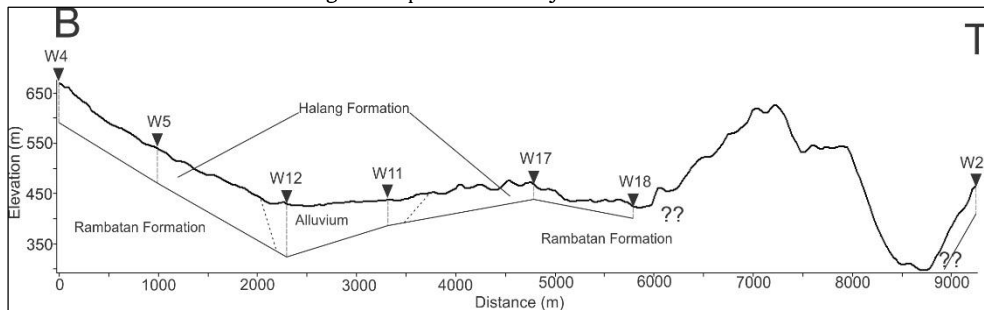


Fig. 7. B-T cross section

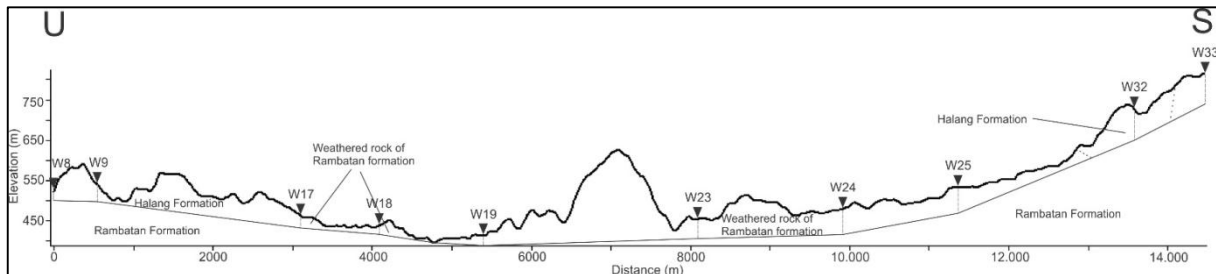


Fig. 8. U-S cross section

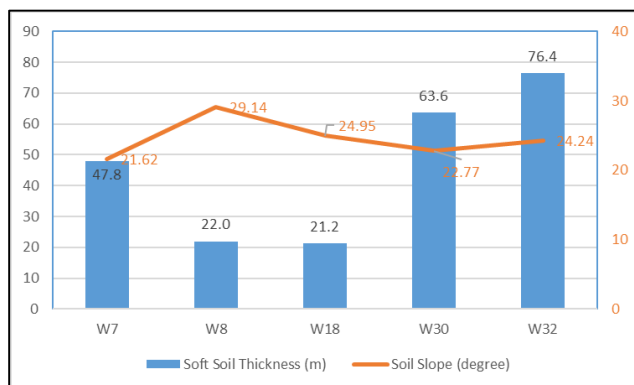


Fig. 9. Soft soil thicknes and soil slope (> 20°)

5. Conclusion

The microtremor can be used to determine the thickness of the soft soil which can provide a preliminary picture of the volume of the soft soil and the morphology of the slip plane. The potential landslide area is an area with thick soft soil and a large soil slope.

The soft layer thickness value in this study is calculated based on the first peak HVSR curve which describes the thick soft layer, which ranges from 17.58 - 103.60 meters. Areas that have the potential for landslides are located at W7, W8, W18, W30 and W32.

In further research, it is necessary to measure using other geophysical methods such as geoelectricity or masw to map the morphology of the slip plane in more detail. In addition, research on soft

soil types is also important so that it can explain the mechanism of landslides that can occur.

Acknowledgements

Acknowledgements are given to DRPM DIKTI who has funded this research through PDP (Penelitian Dosen Pemula) scheme.

References

- Anggono, T., Syuhada, Hananto, N.D., Handayani, L., 2016. Site Response Characteristics of Simeulue Island, Indonesia as Inferred from H / V Spectral Ratio of Ambient Noise Records. *J. Math. Fundam. Sci.* 48, 130–142. <https://doi.org/10.5614/j.math.fund.sci.2016.48.2.4>
- Darsono, Nurlaksito, B., Legowo, B., 2016. Identifikasi Bidang Gelincir Pemicu Bencana Tanah Longsor Dengan Metode Resistivitas 2 Dimensi Di Desa Pablengan Kecamatan Matesih Kabupaten Karanganyar. *Indones. J. Appl. Phys.* 2, 51. <https://doi.org/10.13057/ijap.v2i02.1292>
- Daryono, Sutikno, Sartohadi, J., Dulbahri, Brotopuspito, K.S., 2009. Efek Tapak Lokal (Local Site effect) di Graben Bantul Berdasarkan Pengukuran Mikrotremor, in: *International Conference Earth Science and Technology*. pp. 4–9.
- Djuri, M., Samodra, H., Amin, T., Gafoer, S., 1996. *Geological Map of Purwokerto and Tegal Quadrangles, Java. Bandung.*
- Firmansyah, Feranie, S., Tohari, A., Latief, F.D.E., 2016. Prediction of landslide run-out distance based on slope stability analysis and center of mass approach. *IOP Conf. Ser. Earth Environ. Sci.* 29. <https://doi.org/10.1088/1755-1315/29/1/012003>
- Islami, N., 2019. The Weak Soil Investigation at the Slope Zone in the Hot Spring Area, Rokan Hulu, Indonesia. *J. Geosci. Eng. Environ. Technol.* 4, 236–241. <https://doi.org/10.25299/jgeet.2019.4.4.4258>
- Kamarudin, A.F., Daud, M.E., Ibrahim, Z., Ibrahim, A., 2016. Sustainable Non-destructive Technique Ambient Vibrations for Ground Assessments, in: *Procedia - Social and Behavioral Sciences*. Elsevier B.V., pp. 701–711. <https://doi.org/10.1016/j.sbspro.2015.12.064>
- Koesuma, S., Ridwan, M., Nugraha, A.D., Widiyantoro, S., 2017. Preliminary Estimation of Engineering Bedrock Depths from Microtremor Array Measurements in Solo, Central Java, Indonesia. *J. Math. Fundam. Sci.* 49, 306–320. <https://doi.org/10.5614/j.math.fund.sci.2017.49.3.8>
- Kyaw, Z.L., Pramumijoyo, S., Husein, S., Fathani, T.F., Kiyono, J., 2015. Seismic Behaviors Estimation of the Shallow and Deep Soil Layers Using Microtremor Recording and EGF Technique in Yogyakarta City, Central Java Island, in: *Procedia Earth and Planetary Science*. pp. 31–46. <https://doi.org/10.1016/j.proeps.2015.03.024>
- Liu, L., Weijun, Q.C., Rohrbach, E., 2014. Ambient noise as the new source for urban engineering seismology and earthquake engineering : a case study from Beijing metropolitan area. *Earthq. Sci.* 27, 89–100. <https://doi.org/10.1007/s11589-013-0052-x>
- Méric, O., Garambois, S., Malet, J.P., Cadet, H., Guéguen, P., Jongmans, D., 2007. Seismic noise-based methods for soft-rock landslide characterization. *Bull. la Soc. Geol. Fr.* 178, 137–148. <https://doi.org/10.2113/gssgfbull.178.2.137>
- Naing, T., Pramumijoyo, S., Kawase, H., 2015. Estimation of S-Wave Velocity Structures in Yogyakarta Basin, Indonesia. *J. Appl. Geol.* 1, 60–77. <https://doi.org/10.22146/jag.7228>
- Nakamura, Y., 2008. on the H / V Spectrum. *Proc. 14th world Conf. Earthq. Eng.*
- Okada, H., 2003. *The Microtremor Survey Method (Geophysical Monograph Series No. 12)*. Society of Exploration Geophysicists, Tulsa.
- Prabowo, U.N., Amalia, A.F., Nurdianto, H., Rohim, R., 2019. Microtremor and Slope Data of Watukumpul, Pemalang Regency for Landslide Potential Analysis using Simple Additive Weight Method, in: Setiadi, R.B., Nurdianto, H., Prabowo, U.N. (Eds.), *International Conference on Science & Technologies for Internet of Things*. EAI, Yogyakarta. <https://doi.org/10.4108/eai.19-10-2018.2281299>
- Prabowo, U.N., Amalia, A.F., Wiranata, F.E., 2018. Local site effect of soil slope based on microtremor measurement in Samigaluh, Kulon Progo Yogyakarta. *Local site effect of soil slope based on microtremor measurement in Samigaluh, Kulon Progo Yogyakarta. J. Phys. Conf. Ser.* 1–7.
- Seht, M.I., Wohlenberg, J., 1999. Microtremor Measurements Used to Map Thickness of Soft Sediments. *Bull. Seismol. Soc. Am.* 89, 250–259.
- SESAME European Research Project, 2004. *Guidelines For The Implementation Of The H / V Spectral Ratio Technique On Ambient Vibrations Measurements, Processing And Interpretation.*
- Stanko, D., Markušić, S., Gazdek, M., Sanković, V., Slukan, I., 2019. Assessment of the Seismic Site Amplification in the City of Ivanec (NW Part of Croatia) Using the Microtremor HVSr Method and Equivalent-linear Site Response Analysis. *Geoscience* 9, 1–25. <https://doi.org/10.3390/geosciences9070312>
- Suhendra, Zul Bahrum, C., Sugianto, N., 2018. Geological condition at landslides potential area based on microtremor survey. *ARPN J. Eng. Appl. Sci.* 13, 3007–3013.
- Sulistiaawan, H., Supriyadi, I Yulianti, 2017. Seismic Hazard Analysis based on Earthquake Vulnerability and Peak Ground Acceleration using Microseismic Method at Universitas Negeri Semarang. *J. Phys. Conf. Ser.* 1–7. <https://doi.org/10.1088/1742-6596/755/1/011001>
- Supriyadi, Hidayatullah, R.H., Mahardika, Kusumawardani, R., Upomo, T.C., 2019. Landslide potency based on microseismic data-case study in Trangkil area Gunungpati, Semarang. *J. Phys. Conf. Ser.* 1170. <https://doi.org/10.1088/1742-6596/1170/1/012073>

- Thein, P.S., Pramumijoyo, S., Brotopuspito, K.S., Wilopo, W., Kiyono, J., Setianto, A., 2013. Estimation of Sediment Thickness by Using Microtremor Observations at Palu City , Indonesia, in: The 11th International Conference on Mining, Material and Petroleum Engineering. pp. 21–25.
- Yulianto, G., Harmoko, U., Widada, S., 2016. Identification of Potential Ground Motion Using the HVSr Ground Shear Strain Approach in Wirogomo Area, Banyubiru Subdistrict, Semarang Regency. *Int. J. Appl. Environ. Sci.* 11, 1497–1507.
- Zulfakriza, Z., Puspito, N.T., Nugraha, A.D., Pranata, B., Rosalia, S., 2019. Preliminary Results of Horizontal to Vertical Spectral Ratio (HVSr) Across Lembang Fault, Bandung, Indonesia. *IOP Conf. Ser. Earth Environ. Sci.* 273, 0–6. <https://doi.org/10.1088/1755-1315/273/1/012020>



© 2021 Journal of Geoscience, Engineering, Environment and Technology. All rights reserved. This is an open access article distributed under the terms of the CC BY-SA License (<http://creativecommons.org/licenses/by-sa/4.0/>).